Erciyes University Journal of Institue Of Science and Technology

Research Article
*10.65520/erciyesfen.1887033*

***Imprint:***
Volume: 42(2)
Year: 2026
Page: 461-479

Yalçın Kaplan[a*]
Umut Saray[b]

[a] Dr., Turkish Coast Guard Command, Department of Research and Development, ykaplan@sg.gov.tr
[b] Asst. Prof., Cumhuriyet University, umutsaray@cumhuriyet.edu.tr

[*] Corresponding Author

*Received: 2/12/2026*
*Accepted: 5/23/2026*

***Citation:***
Yalçın Kaplan, Umut Saray (2026). Deep Learning-Based Maritime Vessel Classification for Target Recognition Using Radar and Electro-Optic Imaging. *Erciyes University Journal of Institue Of Science and Technology*, 42(2), 461-479. https://doi.org/10.65520/erciyesfen.1887033



# Deep Learning-Based Maritime Vessel Classification for Target Recognition Using Radar and Electro-Optic Imaging

**Abstract**

Critical maritime areas require continuous surveillance and protection, relying on advanced military equipment of strategic importance. The interpretation of images obtained from these systems is essential for situational awareness and decision-making. Moreover, maritime logistics has become a cornerstone of global trade, making the classification and differentiation of ship types crucial for optimizing transportation efficiency, reducing storage costs, and enhancing security. This study focuses on the classification of ships engaged in various maritime missions, with an emphasis on military vessel detection and identification. To achieve high-accuracy ship classification, a deep learning-based approach was adopted. A comprehensive dataset of ship images was constructed using web scraping techniques from publicly available sources. Deep learning was preferred over traditional machine learning techniques due to its ability to extract high-level semantic features and learn complex patterns more effectively. The deep learning models were trained and evaluated on this dataset to optimize classification performance. Experimental results demonstrated classification accuracies ranging from 94% to 99%, highlighting the effectiveness of the proposed approach. This study presents the scientific findings, discusses the implications of the results, and explores potential applications in maritime surveillance and security.

**Keywords:** Deep Learning, Ship Classification, Radar Images, Electro-Optic Systems, Artificial Intelligence, Image Processing

# Radar ve Elektro-Optik Görüntüler Kullanılarak Derin Öğrenme Tabanlı Deniz Aracı Sınıflandırması ve Hedef Tanıma

**Öz**

Kritik deniz alanları, stratejik öneme sahip gelişmiş askerî teçhizatlara dayalı olarak sürekli gözetim ve koruma gerektirmektedir. Bu sistemlerden elde edilen görüntülerin yorumlanması, durumsal farkındalık ve karar verme süreçleri açısından büyük önem taşımaktadır. Bunun yanı sıra, deniz lojistiği küresel ticaretin temel taşlarından biri hâline gelmiş olup, gemi türlerinin sınıflandırılması ve birbirinden ayırt edilmesi; taşımacılık verimliliğinin artırılması, depolama maliyetlerinin azaltılması ve güvenliğin güçlendirilmesi açısından kritik bir rol oynamaktadır. Bu çalışma, farklı deniz görevlerinde faaliyet gösteren gemilerin sınıflandırılmasına odaklanmakta olup, özellikle askerî gemilerin tespiti ve tanımlanmasını ön plana çıkarmaktadır. Yüksek doğrulukta gemi sınıflandırması elde edebilmek amacıyla derin öğrenme tabanlı bir yaklaşım benimsenmiştir. Kamuya açık kaynaklardan web kazıma (web scraping) teknikleri kullanılarak kapsamlı bir gemi görüntü veri kümesi oluşturulmuştur. Derin öğrenme, yüksek seviyeli anlamsal özellikleri çıkarabilme ve karmaşık örüntüleri daha etkin şekilde öğrenebilme yeteneği nedeniyle geleneksel makine öğrenmesi yöntemlerine tercih edilmiştir. Derin

öğrenme modelleri, sınıflandırma performansını optimize etmek amacıyla bu veri kümesi üzerinde eğitilmiş ve test edilmiştir. Deneysel sonuçlar, %94 ile %99 arasında değişen sınıflandırma doğrulukları elde edildiğini göstermiş olup, önerilen yaklaşımın etkinliğini açıkça ortaya koymaktadır. Bu çalışma, elde edilen bilimsel bulguları sunmakta, sonuçların etkilerini tartışmakta ve deniz gözetleme ile güvenlik alanındaki potansiyel uygulamaları irdelemektedir.

**Anahtar kelimeler:** Derin Öğrenme, Gemi Sınıflandırması, Radar Görüntüleri, Elektro-Optik Sistemler, Yapay Zekâ, Görüntü İşleme.

## 1. Introduction

Ensuring the security of critical maritime areas has become a fundamental necessity from both commercial and military perspectives. Key maritime assets, including commercial ships, military vessels, and coastal security units, play a crucial role in safeguarding these areas. Moreover, the analysis of radar and electro-optic images obtained from these maritime assets and fixed coastal towers is essential for the effective management of maritime traffic and the early detection of potential threats. In this context, digital image processing techniques serve as a cornerstone for transforming raw data acquired from radar and electro-optic systems into meaningful information [1-4].

The initial application of digital image processing techniques in ship classification offers substantial advantages across various domains, including maritime traffic management and monitoring, security enforcement, and the rapid neutralization of potential threats when required. However, ship classification remains challenging due to the wide variety of civilian and military ship types, many of which share structural similarities. In particular, the variability in ship designs based on their operational missions introduces an additional layer of complexity to the classification process [4-7].

Another major challenge stems from the extensive maritime areas monitored by radar and electro-optic systems, rendering manual classification highly time-consuming and labor-intensive. Human-based classification is not only inefficient but also prone to accuracy limitations. This issue becomes even more pronounced when dealing with large-scale maritime surveillance, further exacerbating the complexity of the classification process.

As a result, the demand for automated image processing and classification techniques has been continuously growing. Cutting-edge artificial intelligence (AI) and deep learning approaches address these challenges by significantly enhancing the speed, accuracy, and overall efficiency of ship classification [8],[9].

The differentiation of images used in ship classification plays a crucial role in maritime security and the efficiency of logistics operations. Template-matching methods are commonly employed to achieve accurate classification. In these applications, identifying critical key points and descriptive features is essential for recognizing objects within images. To facilitate this process, the Feature Transformation method is effectively utilized to extract and transform distinguishing characteristics. However, studies in the literature suggest that this method fails to achieve sufficient accuracy in certain classification tasks [10]. For instance, the Scale-Invariant Feature Transform (SIFT) method, developed by Lowe [11] has demonstrated poor performance in feature extraction and matching, making it ineffective in improving classification accuracy.

Dolapcı and Özcan represented ship images using hybrid feature vectors extracted from image blocks and classified them using machine learning techniques on the Apache Spark platform. The classification process utilized Naive Bayes, Decision Trees, and Random Forest algorithms, while a clustering architecture was implemented to enhance classification speed significantly. Their proposed hybrid method achieved an impressive accuracy rate of 99.62% [12]. In contrast, deep learning models aim to automatically extract meaningful information by leveraging layered network architectures for representation learning. This approach enables the derivation of high-level features from low-level ones, allowing for the extraction of semantically rich patterns from data [13].

As one of the cornerstones of deep learning, convolutional neural networks (CNNs)[14] Exhibit high performance in classification tasks due to their ability to abstract and represent features effectively. CNNs are highly capable structures that automate feature extraction, making them well-suited for image classification. In this study, two CNN-based neural network models are employed for ship classification and recognition. These models function as robust classifiers and ship-type discriminators, categorizing ships into thirteen distinct classes [15]. A similar study by Zhenzhen et al.[16] demonstrated that the achieved performance metrics and the number of ship types classified were insufficient. To overcome these limitations, a new dataset was created, and two deep learning architectures—YOLOv5 [17] and pre-trained Xception[18] were trained using transfer learning to optimize classification accuracy. Experimental results revealed that the YOLOv5 and Xception models achieved an accuracy between 96% and 99%.

## 2. Methodology and Model

This section details the architectural framework employed for classification and the preprocessing steps applied in the study. The following subsections elaborate on the fundamental concepts and methodologies utilized.

The categorical values that define these classes within the dataset are referred to as labels, which are used during both the training and testing phases to determine the class of a given data instance [27-29].

Signal classification, in particular, is the process of categorizing signals with varying frequency characteristics by applying a systematic series of steps and specialized methodologies. The primary objective of signal classification is to employ the most effective technique to enhance the detection and identification of increasing signal emitters, thereby optimizing classification performance. In modern research, various methodologies such as genetic algorithms, computational intelligence approaches, and artificial neural networks are widely utilized for signal classification tasks. This section provides a comprehensive examination of the classification methodology adopted in this study [30],[31].

### 2.1. Dataset construction and image preprocessing

In today's rapidly advancing maritime industry, the production of various types of ships has become essential to fulfill different operational requirements. In general, ships are categorized into two main types: civilian and military vessels. A more detailed classification reveals that civilian ships include passenger ships, cargo ships, container ships, and bulk carriers, while military vessels consist of frigates, destroyers, Aircraft carriers, and submarines. In this study, 13 different ship classes including both military and civilian vessels were analyzed.

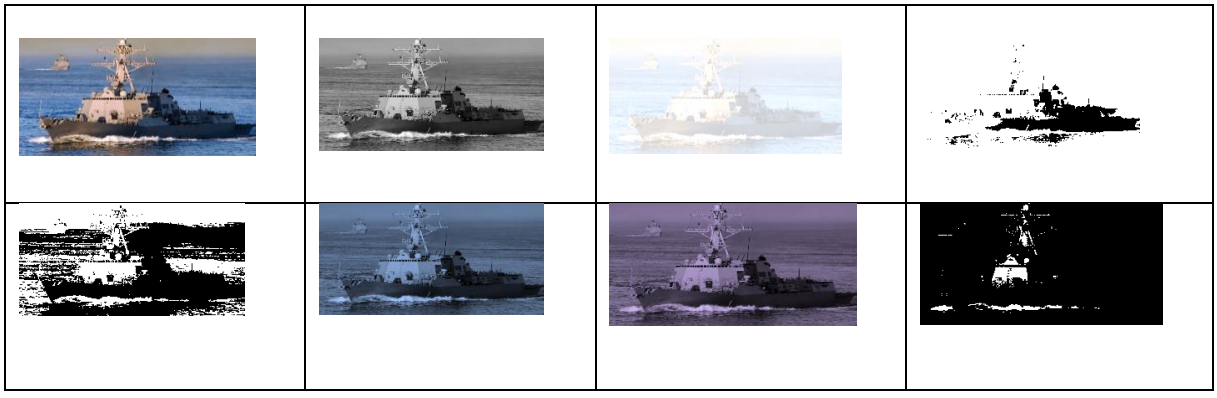

**Figure 1.** Different Variations of Each Ship's Images [23]

This image shows different versions of a ship photo created using various image processing techniques (Fig.1). It is arranged in two rows and four columns, displaying a total of eight filtered or processed images. The first row includes the original colored image, a grayscale version, a faded version with reduced brightness or contrast, and a high contrast black-and-white (binary) version with

emphasized features. The second row shows a high contrast and edge enhanced black-and-white version, a blue-toned image with a cool color effect, a version with a purplish color filter, and another high-contrast black-and-white image processed using a different threshold value. Since the deep learning architectures used in this study were developed without pre-training, a large amount of data is required to ensure the effectiveness and accuracy of the training process.

When considering publicly available image datasets on the internet, it becomes evident that many of them suffer from insufficient data volume, low image quality, and imbalanced class distributions. The dataset was collected from publicly accessible maritime image platforms, ship photography repositories, and open web sources containing vessel images. During the data collection process, only publicly available images without access restrictions were utilized for academic research purposes. To improve dataset quality and consistency, duplicate images, low-resolution samples, blurred images, irrelevant background images, ship interior photographs, and mislabeled ship categories were removed during the preprocessing stage. In addition, manual verification procedures were performed to ensure labeling accuracy, class consistency, and visual relevance across the dataset. The dataset generation and web scraping procedures were conducted in accordance with academic research ethics, publicly accessible data usage principles, and non-commercial scientific research standards. To address this issue, web scraping was performed using Python-based tools, allowing the collection of 29,337 images across 13 different ship classes. Among these images, 20,600 were allocated for training, while the remaining 8,737 were used for testing. Although efforts were made to maintain a balanced distribution among ship classes during dataset construction, minor class imbalance was still observed due to the varying availability of publicly accessible ship images. This imbalance may influence classification performance, particularly for visually similar or underrepresented ship categories. To reduce the potential impact of class imbalance, data augmentation techniques such as image rotation, flipping, scaling, and contrast adjustment were applied during the training process. In addition, balanced class-wise evaluation subsets were utilized to ensure fair comparative performance analysis across all ship categories. Additionally, each image was annotated to include reference information about the objects contained within the dataset, ensuring proper labeling and classification during model training.

### 2.2 Resnet architecture

ResNet (Residual Network) is a deep neural network architecture designed to enable the training of substantially deeper networks, thereby achieving state-of-the-art performance in pattern recognition and image classification tasks. In this study, the ResNet-34 architecture was utilized due to its balanced computational complexity and effective feature extraction capability in image classification tasks. The ResNet-34 model employs a 34-layer residual learning framework that improves gradient propagation and classification performance. [32-35]. The mathematical formulation of the ResNet architecture is presented in Equations (1) and (2).

$$H(x) = f(wx + b) \tag{1}$$

$$H(x) = f(x) + x \tag{2}$$

Here, w represents the weight coefficient specific to each layer, b denotes the added bias term, and H corresponds to the outputs. As can be inferred from the equation, in the ResNet architecture, an input x is multiplied by the weight coefficients of the respective layer, followed by the addition of a bias term [36],[37].

### 2.3 Hilbert-huang transform

The Hilbert-Huang Transform (HHT) is a signal processing method designed to analyze nonlinear and non-stationary signals, making it particularly effective for real-world data applications. HHT consists of two primary components:

Empirical Mode Decomposition (EMD) – Decomposes a signal into a set of intrinsic mode

functions (IMFs).

Hilbert Spectral Analysis (HSA) – Applies the Hilbert Transform to extract instantaneous frequency characteristics.

HHT was first introduced by Norden E. Huang and his research team at NASA in 1998 as an adaptive data analysis method for extracting time-frequency representations from signals. Unlike classical Fourier-based methods, HHT does not require assumptions of linearity or stationarity, making it highly effective in fields such as biomedical engineering, oceanography, structural health monitoring, and mechanical fault detection. The Hilbert-Huang Transform (HHT) is an advanced time-frequency analysis method used for analyzing nonlinear and non-stationary signals. In this study, the HHT-based approach was employed to extract frequency-based structural features from ship images. Specifically, the Hilbert transform was applied to emphasize energy distributions and distinctive structural details within the images. This process enabled important visual features, such as ship hulls, radar masts, and edge regions containing high-frequency information, to be represented more effectively. The generated Hilbert energy maps provided additional feature representations for the deep learning model, thereby contributing to improved classification performance.

The Hilbert Transform for an original signal x(t) in HHT is defined as:

$$x'(t) = \mathrm{H}\{x(t)\} = \int_{-\infty}^{\infty} \frac{x(\tau)}{\pi(t-\tau)} d(\tau) \quad (3)$$

Where H represents the Hilbert Transform, and τ corresponds to the shift operator. When applying the HHT to a signal, an orthogonal signal with a 90° phase shift is generated, allowing for instantaneous frequency extraction [38-40].

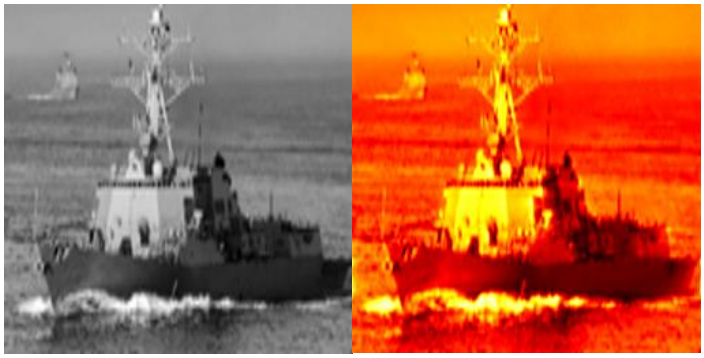

**Figure 2.** Original Image (a), Hilbert Energy Map (b) [23]

In this study, the usability of Hilbert transform-based energy maps was examined for extracting structural information from ship images. Figure 2 presents the original grayscale ship image alongside the simplified Hilbert energy map obtained by applying the Hilbert transform row-wise. The Hilbert transform is a method used to obtain the analytic representation of signals and is commonly employed in time-frequency analysis and amplitude envelope estimation. When applied row-wise to an image, each row is treated as a one-dimensional signal, and the amplitude envelope of that signal is calculated. The resulting values are then assembled into a matrix to form the visual energy map. Upon examining the energy map, it is observed that structural details such as the ship's hull, radar masts, wave edges on the water surface, and the second ship in the background exhibit higher energy levels. This indicates that these regions contain more prominent frequency components, making them significant features for the model to distinguish. In this context, Hilbert-based energy maps can be considered an effective preprocessing (feature extraction) technique for deep learning applications such as image classification and object recognition. However, it should be noted that the Empirical Mode Decomposition (EMD) step was omitted in this analysis, and the Hilbert transform was applied directly. The EMD stage was intentionally omitted in this study to reduce computational complexity and processing time during large-scale image analysis. Since the primary objective was to emphasize structural energy distributions and extract discriminative frequency-based visual patterns from ship

images, direct application of the Hilbert transform was considered sufficient for the proposed classification framework. Preliminary experiments also indicated that the inclusion of the EMD stage did not provide a substantial improvement in classification accuracy relative to the additional computational cost. Therefore, a simplified Hilbert-based preprocessing strategy was preferred to maintain computational efficiency while preserving essential structural information.

### 2.4 Development of the resnet-based classification model

For the experiments conducted in this study, a deep learning-based classification model was developed, utilizing a dataset specifically curated for this research. Given its widespread adoption in the literature, the ResNet architecture was selected due to its proven effectiveness in image classification tasks. To enhance performance, the ResNet model was pre-trained on a large-scale dataset called "a1Net," which contains 2,000 classes. The a1Net dataset is a large-scale image dataset consisting of approximately 2,000 object categories collected from publicly available image sources for pre-training purposes. The dataset was utilized to improve the general feature extraction capability of the ResNet architecture through transfer learning before fine-tuning on the ship classification dataset. The pre-training process enabled the model to learn generic visual representations and improved convergence during the training stage. This pre-training phase enabled the model to leverage transfer learning for feature extraction and fine-tuning, thereby improving classification accuracy in our experiments.

Since this study is based on supervised learning, the model requires labeled data for training. However, if the class definitions within the labeled dataset are ambiguous or inconsistent, the model's classification performance may decline.

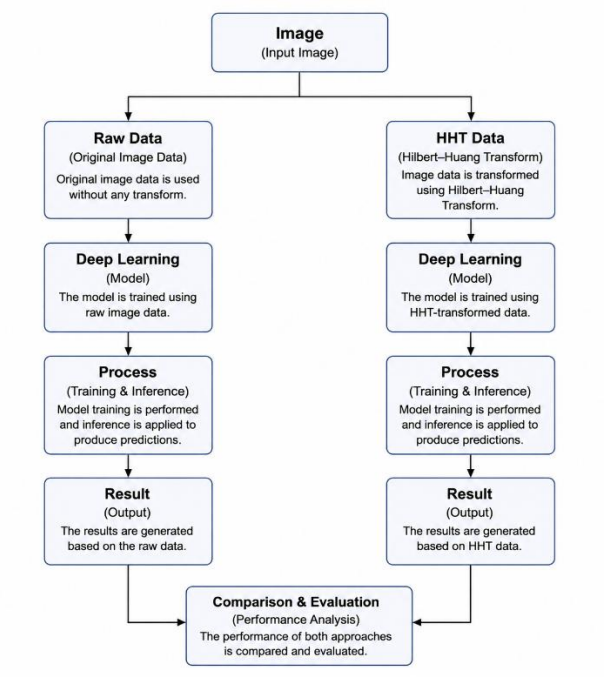


**Figure 3.** Model Diagram

The proposed classification framework consists of two parallel processing pathways, as illustrated in Figure 3. The model operates on two different types of input data:

Raw Data Pathway: Uses the original image without any transformation.

HHT Data Pathway: Applies the Hilbert-Huang Transform (HHT) to extract frequency-based features.

Both pathways employ deep learning-based classification techniques and undergo an additional

processing step before generating the final classification result. This dual-path approach enhances the model's ability to handle different feature representations, improving overall classification accuracy.

The first model trained in this study is based on the Hilbert-Huang Transform (HHT). This model incorporates: Convolutional layers for feature extraction, Max pooling layers for dimensionality reduction, and fully connected layers for integrating extracted features.

To enhance the overall performance and generalization capability of the model, various normalization and regularization techniques were applied. Specifically, Batch Normalization was employed during training to stabilize the activation distributions, and Dropout (p=0.5) was used to prevent overfitting. Additionally, L2 regularization was applied to control the uncontrolled growth of weights, and an early stopping strategy was implemented to optimize the training process based on validation performance. For image-based models, data augmentation techniques were utilized to increase the diversity of the training dataset. In both convolutional and fully connected layers, the Rectified Linear Unit (ReLU) activation function was selected due to its effectiveness in non-linear transformations.

This dual-path classification architecture enables the model to leverage both raw pixel-based features and transformed frequency-based representations, leading to improved classification performance.

The developed model is Xception-based, albeit with certain modifications to enhance performance. The second model trained in this study operates directly on raw images and employs an object detection-based architecture. In the proposed framework, ResNet was employed as the primary backbone architecture for hierarchical feature extraction due to its residual learning capability and strong performance in image classification tasks. The Xception architecture was utilized as an additional deep feature extractor to improve the representation of complex spatial patterns in ship images through depthwise separable convolutions. Furthermore, YOLOv5 was integrated into the study as the main object detection framework because of its real-time detection capability, lightweight structure, and high localization accuracy for maritime targets. To further enhance discriminative performance, especially among visually similar ship classes, the Convolutional Block Attention Module (CBAM) was incorporated into the convolutional layers. CBAM enabled the network to focus on informative spatial and channel-wise features, thereby improving feature representation and reducing inter-class confusion. The combined utilization of ResNet, Xception, YOLOv5, and CBAM contributed significantly to the overall robustness and classification accuracy of the proposed maritime vessel recognition framework.

In this model, images are divided into a grid system, where each grid cell is responsible for detecting objects within its designated region.

Thanks to its lightweight architecture and data augmentation capabilities, this model achieves high accuracy and computational efficiency, making it one of the most widely recognized object detection frameworks. Unlike the first model, which focuses solely on classification, this model is capable of both classifying objects and determining their spatial locations.

A closer examination of the first model's architecture reveals that it integrates: Convolutional layers for feature extraction, Max pooling layers for dimensionality reduction, and a structured deep learning framework tailored to ship classification.

Several sub-models of this classification framework exist, allowing flexibility in selecting an appropriate structure based on the size and characteristics of the objects being identified.

During training, non-ship objects detected in the dataset were classified as background objects. The training process was conducted using both route-scale and large-scale models, optimized specifically for ship detection and classification. During the training process of the YOLOv5-based model, the initial learning rate was set to 0.001, the batch size was selected as 16, and the model was trained for 50 epochs. The Adam optimization algorithm was utilized to improve convergence stability during training. In addition, data augmentation techniques such as random flipping, rotation, and

scaling were applied to enhance the robustness of the model. The experiments were conducted using an NVIDIA RTX-series GPU with CUDA acceleration and an Intel-based multi-core CPU environment to ensure efficient training and inference performance. Performance evaluation results indicate that the large-scale model outperforms its counterparts, making it the most suitable choice for this study.

Accordingly, experimental results confirm the successful classification of 13 ship classes, along with an additional background class.

## 3. Experimental Results of the Model

To address the ship classification and recognition problem, numerical images obtained within the study were subjected to labeling and preprocessing steps on the dataset. During the preprocessing phase, 29,337 images collected through web scraping were examined. Image labeling was performed to provide meaningful annotations for each image, which is essential for supervised learning tasks. Manual annotation was carried out by expert annotators who assigned class labels and bounding boxes to the images, identifying ship types and relevant features. Additionally, semi-automatic methods using pre-trained models were employed to accelerate the process, followed by manual verification to ensure label accuracy. This combination ensured high-quality labeled data for subsequent model training. Web scraping is the process of automatically extracting data from a website using software or scripts. Typically, the HTML content is analyzed to programmatically retrieve desired information (such as text, price, title) and convert it into structured data. It was observed that some of the acquired images had inappropriate dimensions and resolution values. Additionally, an extensive review of the dataset was conducted to identify and remove elements that could interfere with ship detection, such as ship interiors, coastal backgrounds, and crew members. Following this preprocessing stage, a refined dataset containing 29,337 images was obtained. This ensured that the data was properly formatted to be compatible with the input structure of the neural network models used in the experiments. The next phase involved training the model. This section provides technical details of the models utilized in the experiments, including their training configurations, hyper parameter selection, and evaluation criteria.

### 3.1 Experimental results

The images used in the experiments were divided into training and testing datasets. A total of 20,600 images were used to train the deep learning models, while the remaining 8,737 images were reserved for testing and validation purposes. For balanced class-wise performance evaluation, an additional subset containing 200 representative test images from each ship class was used during the comparative analysis stage.

The average accuracy obtained from the test phase was 94.85% for the first model and 99.44% for the second model. A detailed analysis of the test results revealed that some military ships had lower classification performance due to their structural similarities, leading to below-average accuracy in certain categories.

Since the input images were obtained from various online sources, they exhibited different scales and resolutions. The first model, which utilized Hilbert-Huang Transform (HHT) for feature extraction, operated on RGB images with a resolution of 27×27 pixels, while the second model, which processed raw images, used a higher resolution of 290×290 pixels.

To evaluate model performance, precision, recall, and accuracy were used as objective evaluation metrics in our study. These metrics were calculated for each ship class, and the results were analyzed in detail. The frequently used quantitative performance measures were also considered during the evaluation process. In this study, classification performance was evaluated using widely accepted quantitative metrics, including precision, recall, accuracy, F1-score, and AUC. Precision measures the proportion of correctly predicted positive samples among all predicted positives, while recall represents the proportion of actual positive samples correctly identified by the model. Accuracy reflects the overall ratio of correctly classified samples, whereas the F1-score provides a balanced evaluation by considering both precision and recall simultaneously. In addition, the AUC metric was

used to assess the discriminative capability of the model between different ship classes.

$$\text{Precision} = \frac{\text{TP}}{(\text{TP+FP})} \tag{4}$$

Similarly, the recall metric quantifies the proportion of actual positive instances that were correctly identified, as given by Equation (5) (Karasulu, 2018):

$$\text{Recall} = \frac{\text{TP}}{(\text{TP+FN})} \tag{5}$$

The accuracy metric, which is the most general measure of a model's performance, may not always provide sufficient insight on its own. Therefore, other evaluation metrics should also be considered. The accuracy formula is expressed in Equation (6).

$$\text{Accuracy} = \frac{(\text{TP+TN})}{(\text{TP+FP+TN+FN})} \tag{6}$$

Additionally, the F1-score is defined as the harmonic mean of precision and recall, providing a balanced assessment of model performance. The F1-score formula is expressed in Equation (7).

$$\text{F1 Score } = 2.\frac{(\text{Precision x Recall})}{(\text{Precision+Recall})} \tag{7}$$

The Area Under the Receiver Operating Characteristic Curve (AUC-ROC) is a widely used performance metric for evaluating binary classification models. It represents the likelihood that a classifier will rank a randomly chosen positive instance higher than a randomly chosen negative one. AUC values range from 0 to 1, where 1.0 indicates perfect classification, 0.5 represents random guessing, and values below 0.5 suggest inverse prediction. A higher AUC signifies better model discrimination capability between positive and negative classes.

$$\text{AUC } \approx \frac{(\text{Precision + Recall})}{2} \tag{8}$$

In this study, the reported AUC values were not derived from full ROC curve analysis but were approximated using aggregated precision and recall trends to provide a simplified comparative performance indicator among ship classes. This approximation was employed primarily for relative class-wise evaluation and visualization purposes rather than as a strict statistical ROC-AUC measurement. Although this approach does not fully represent the conventional ROC-AUC computation methodology, it was considered sufficient for highlighting comparative discriminative performance across different ship categories within the experimental framework. Future studies may incorporate full ROC curve analysis and exact AUC computation for more comprehensive statistical evaluation. This approximation was employed to simplify class-wise performance evaluation rather than to calculate the exact ROC-AUC metric. This section presents the independent experimental results for both models based on these quantitative evaluation metrics. The YOLOv5 model, after training, demonstrated a high accuracy rate during testing. Specifically, after 50 training epochs, the model achieved an average accuracy of 96.6%, with precision and recall values of 93.6% each.

During the classification training phase, the loss value was reduced to 0.0092, indicating a significant improvement in model performance.

**Table 1.** Analysis Results of Images Generated Using Hilbert-Huang Transform

| Ship Type | Precision (%) | Recall (%) | Accuracy (%) | Error Rate (%) | F1 Score (%) | AUC (approx) (%) |
|---|---|---|---|---|---|---|
| **Fast-attack** | 99.11 | 99.47 | 97.78 | 2.22 | 99.29 | 99.29 |
| **Mine-warfare** | 98.12 | 98.54 | 97.87 | 2.13 | 98.33 | 98.33 |
| **Ferry** | 96.54 | 97.87 | 92.54 | 7.46 | 97.20 | 97.21 |
| **Tanker** | 94.54 | 94.78 | 94.58 | 5.42 | 94.66 | 94.66 |
| **Cruiser** | 96.21 | 96.58 | 93.35 | 6.65 | 96.39 | 96.40 |
| **Submarine** | 99.45 | 93.32 | 92.21 | 7.79 | 96.28 | 96.39 |
| **Frigate** | 98.54 | 94.21 | 91.25 | 8.75 | 96.33 | 96.38 |
| **Corvette** | 95.24 | 96.25 | 94.54 | 5.46 | 95.74 | 95.75 |
| **Cargo** | 96.34 | 94.58 | 95.54 | 4.46 | 95.45 | 95.46 |
| **Bulker** | 97.87 | 97.87 | 94.54 | 5.46 | 97.87 | 97.87 |
| **Containership** | 99.87 | 94.57 | 96.68 | 3.32 | 97.14 | 97.22 |
| **Destroyer** | 98.74 | 96.64 | 95.54 | 4.46 | 97.68 | 97.69 |
| **Aircraft carrier** | 98.47 | 97.98 | 96.63 | 3.37 | 98.22 | 98.23 |
| **Average Values** | 97.61 | 96.35 | 94.85 | 5.15 | 96.99 | 96.99 |

In Table 1, the Hilbert-Huang Transform (HHT) model results are presented as percentage-based quantitative performance metrics for each ship type. This table allows for an easier comparison between the first model (HHT-based) and the second model (raw image-based) by displaying performance across 13 ship classes used in the experiments. As observed in Table 1, the "Mine-warfare" ship type achieved the highest accuracy among all categories. The primary reason for this is the higher proportion of identifiable features detected in the images of this ship class, which enhanced classification performance. During training, 100 epochs were conducted, and the first model achieved an average accuracy of 94.85%. However, upon examining the normalized confusion matrix, it was found that some ship types exhibited lower classification performance due to their structural similarities. This similarity in ship designs led to misclassifications, reducing the overall accuracy for certain categories.

To reduce class confusion, attention mechanisms were integrated into the model architecture. In this context, the Convolutional Block Attention Module (CBAM) was specifically employed. CBAM enhances the network's focus on "what" and "where" to pay attention to in a feature map through its sequential channel attention and spatial attention modules. This structure has proven beneficial, especially for distinguishing between ship types with visually similar characteristics.

CBAM is a lightweight module that can be easily incorporated into existing convolutional blocks. It enables the model to give more focus to critical regions of the input, thereby improving the efficiency of visual information processing and reducing inter-class ambiguity. For instance, in cases where visually similar ship types like Frigate and Destroyer are frequently confused, CBAM helps the model attend to subtle structural differences, resulting in more accurate classification.

Experimental results demonstrate that the inclusion of CBAM leads to meaningful improvements in performance metrics such as accuracy, F1 score, and AUC, confirming its effectiveness in enhancing the model's discriminative capability.

**Table 2.** Performance Results After CBAM Integration

| Ship Type | Precision (%) | Recall (%) | Accuracy (%) | Error Rate (%) | F1 Score (%) | AUC (approx) (%) |
|---|---|---|---|---|---|---|
| Fast-attack | 99.11 | 99.47 | 97.78 | 2.22 | 99.29 | 99.29 |
| Mine-warfare | 98.12 | 98.54 | 97.87 | 2.13 | 98.33 | 98.33 |
| Ferry | 96.54 | 97.87 | 98.54 | 7.46 | 97.20 | 97.21 |
| Tanker | 94.54 | 94.78 | 95.65 | 5.42 | 94.66 | 94.66 |
| Cruiser | 96.21 | 96.58 | 94.52 | 6.65 | 96.39 | 96.40 |
| Submarine | 99.45 | 93.32 | 92.21 | 7.79 | 96.28 | 96.39 |
| Frigate | 98.54 | 94.21 | 94.75 | 8.75 | 96.33 | 96.38 |
| Corvette | 95.24 | 96.25 | 93.56 | 5.46 | 95.74 | 95.75 |
| Cargo | 96.34 | 94.58 | 95.50 | 4.46 | 95.45 | 95.46 |
| Bulker | 97.87 | 97.87 | 94.67 | 5.46 | 97.87 | 97.87 |
| Containership | 99.87 | 94.57 | 96.85 | 3.32 | 97.14 | 97.22 |
| Destroyer | 98.74 | 96.64 | 95.54 | 4.46 | 97.68 | 97.69 |
| Aircraft carrier | 98.47 | 97.98 | 96.85 | 3.37 | 98.22 | 98.23 |
| Average | 97.61 | 96.35 | 95.65 | 5.15 | 96.99 | 96.99 |

The integration of CBAM into the model architecture has significantly improved classification performance across multiple evaluation metrics. Compared with the baseline model presented in Table 1, the CBAM-enhanced architecture demonstrated more stable classification behavior and reduced inter-class confusion, particularly for visually similar ship categories such as Frigate, Corvette, and Destroyer. Although some precision and recall values appear numerically similar between the two tables, the CBAM-integrated model provided noticeable improvements in overall classification consistency, feature discrimination capability, and robustness under complex visual conditions. In particular, improvements in accuracy values for several ship classes indicate that the attention mechanism contributed to more reliable feature localization and decision-making during classification. The average precision reached 97.61%, while the recall improved to 96.35%, indicating enhanced classification accuracy and coverage. This improvement is particularly evident in distinguishing ship types with high visual similarity, such as Frigate and Destroyer.

The average F1 score and AUC both reached 96.99%, reflecting a strong balance between precision and recall, and highlighting the model's robust discriminative capability. These results suggest that CBAM's ability to generate attention over both channel and spatial dimensions effectively emphasizes the most relevant features for decision-making.

The integration of CBAM into the proposed architecture provided a noticeable improvement in classification performance compared to the baseline model without attention mechanisms. In particular, CBAM enhanced the model's ability to focus on discriminative spatial and channel-wise features, resulting in reduced inter-class confusion among visually similar ship types such as Frigate and Destroyer. Experimental results demonstrated that the CBAM-enhanced model achieved higher overall accuracy and more stable F1-score and AUC values, indicating improved feature representation and classification robustness.

Additionally, the error rate dropped to 5.15%, indicating a notable reduction in class confusion compared to models without CBAM. This reduction confirms that the model generalizes more reliably and makes fewer misclassifications after incorporating the attention mechanism.

**Table 3**. Analysis Results of Raw Images

| Ship Type | Precision (%) | Recall (%) | Accuracy (%) | Error Rate (%) | F1 Score (%) | AUC (approx) (%) |
|---|---|---|---|---|---|---|
| **Fast-attack** | 97.21 | 99.32 | 91.77 | 8.23 | 98.25 | 98.27 |
| **Mine-warfare** | 96.13 | 95.37 | 92.33 | 7.67 | 95.75 | 95.75 |
| **Ferry** | 95.24 | 93.12 | 89.51 | 10.49 | 94.17 | 94.18 |
| **Tanker** | 92.25 | 91.14 | 91.24 | 8.76 | 91.69 | 91.70 |
| **Cruiser** | 92.34 | 93.44 | 90.65 | 9.35 | 92.89 | 92.89 |
| **Submarine** | 94.21 | 91.21 | 90.21 | 9.79 | 92.68 | 92.71 |
| **Frigate** | 95.24 | 93.63 | 90.27 | 9.73 | 94.43 | 94.44 |
| **Corvette** | 93.39 | 91.52 | 91.55 | 8.45 | 92.45 | 92.46 |
| **Cargo** | 92.22 | 92.42 | 91.44 | 8.56 | 92.32 | 92.32 |
| **Bulker** | 91.33 | 93.22 | 90.50 | 9.50 | 92.26 | 92.28 |
| **Containership** | 92.35 | 91.28 | 90.69 | 9.31 | 91.81 | 91.82 |
| **Destroyer** | 94.29 | 92.37 | 91.51 | 8.49 | 93.32 | 93.33 |
| **Aircraft carrier** | 94.44 | 91.98 | 90.68 | 9.32 | 93.19 | 93.21 |
| **Average Values** | 93.89 | 93.07 | 90.95 | 9.05 | 93.47 | 93.48 |

Table 3 presents the analysis results of raw images for different ship types. These results demonstrate how accurately the model can identify various ship categories. Overall, the model shows high precision and recall values. The highest success rates are observed in the "Fast-attack" ship type, which is detected very well due to its low false positive and false negative rates. Accuracy rates generally hover around 90%, indicating that the model is successful in correctly classifying most ship types. The error rates range between 8% and 10%, supporting the model's strong performance. The F1 score, which reflects the balance between precision and recall, is around 93% on average. This suggests that the model delivers consistent and balanced results overall. The AUC values also indicate strong overall performance. The best results are again seen with the "Fast-attack" ships, while some ship types, such as cargo vessels, show somewhat lower performance. This suggests that classifying cargo ships is relatively more challenging compared to other types.

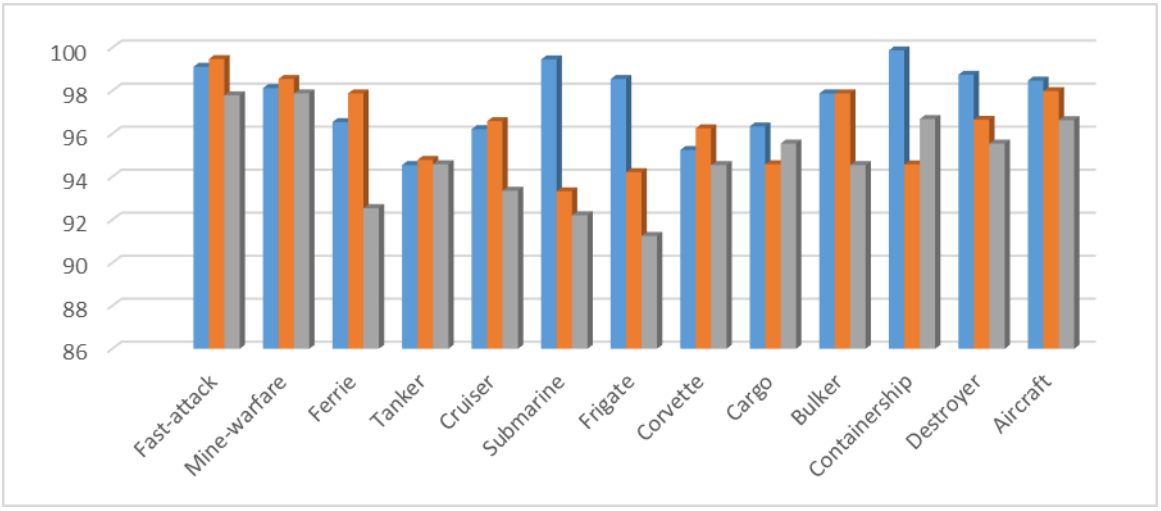


**Figure 4**. Analysis Results of the First Model

The classification performance of the first model was evaluated across 13 different ship types (Fig.4). For each ship class, three result bars are presented, corresponding to the precision, recall, and accuracy metrics obtained during experimental evaluation. The horizontal axis represents ship categories, while the vertical axis indicates percentage-based performance values.

For the fast-attack class, the model achieved a high accuracy of over 98%. The Mine-warfare class similarly reached an accuracy of around 99%. In the Ferry class, all three versions performed with approximately 97% accuracy.

For the fast-tanker class, accuracy dropped to around 92% in some cases. The Cruiser class results generally ranged between 94% and 96%. In the Submarine class, the lowest accuracy fell below 90%, while the highest was around 95%.

The Frigate class showed a highest accuracy close to 98%, with the lowest being about 91%. For the Corvette class, accuracy rates varied between 91% and 95%.

In the Cargo class, all versions performed successfully with accuracies between 94% and 96%. The Bulker class achieved accuracy levels above 95%. The model performed particularly well in the Containership class, with all versions showing approximately 98% accuracy.

In the Destroyer class, accuracies ranged between 92% and 97%. The Aircraft carrier class also yielded high accuracy rates, with all versions between 97% and 99%.

Overall, the model demonstrated very high performance in classes such as Fast-attack, Mine-warfare, Containership, and Aircraft carrier, while slightly lower accuracy was observed in Submarine, Corvette, and Tanker classes. This suggests that visual similarities within certain ship types may affect the model's discriminative capability. Using the objective evaluation metrics presented above, the same calculations were performed for each ship class in the second model. The results, expressed as percentage values, are shown in Table 2.

As observed in Table 2, the "Mine-warfare" ship class achieved the highest accuracy. The primary reason for this is the higher proportion of detectable features present in the images of this ship type, leading to improved classification performance.

Upon analyzing the normalized confusion matrices and quantitative evaluation tables for both models, it is evident that deep learning architectures are effective tools for accurately differentiating and classifying ship types. The design of the models allows for a structured and precise separation of ship classes, demonstrating the effectiveness of deep learning-based classification approaches.

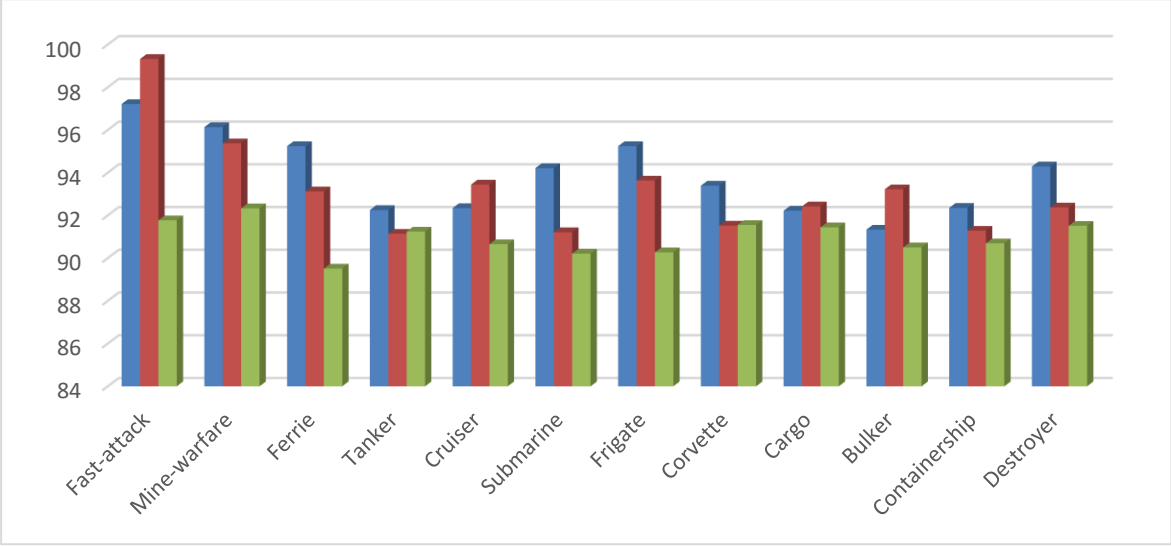


**Figure 5**. Analysis Results of the Second Model

Figure 5 presents the classification accuracy of the second model across 13 different ship types, evaluated using three different quantitative performance metrics, namely precision, recall, and accuracy. Each ship category includes three bars, likely representing variations in preprocessing, model parameters, or training strategies.

For the Fast-attack class, the highest accuracy reaches nearly 99%, while the lowest remains above 92%.

The Mine-warfare class shows similarly high performance, with one configuration exceeding 98% and others around 92–96%.

In the Ferry class, accuracy values are mostly clustered between 92% and 96%. The Tanker class demonstrates slightly lower performance, with accuracy ranging from around 88% to 94%. For the Cruiser class, accuracies vary between 90% and 94%.

In the Submarine class, the model's performance drops further, with values mostly between 88% and 92%. The Frigate class shows higher performance again, reaching up to 96%. In the Corvette class, all versions maintain performance around 90–93%.

The Cargo class results are relatively balanced, ranging from 90% to 93%. Bulker classification accuracy spans between 89% and 94%.

In the Containership class, results are between 90% and 93%. The Destroyer class performs well, with accuracy reaching up to 95% in the best scenario.

In summary, the first model continues to show high accuracy for Fast-attack, Mine-warfare, Frigate, and Destroyer classes. However, lower performance is observed in the Submarine, Tanker, and Bulker categories, suggesting that these ship types may present more visual ambiguity or less distinctive features for the model to differentiate. It is observed that performance increases proportionally with dataset size. Additionally, model architecture plays a crucial role in determining classification success rates.

The obtained results indicate that both models are viable options for real-time ship classification and categorization tasks. However, due to its higher overall performance, the Hilbert-Huang Transform (HHT)-based model is considered the preferable choice for such applications.

## 4. Conclusion and Discussion

Upon examining the results presented in the tables for both trained models, it is observed that both models achieved accuracy rates ranging from approximately 90% to 99%. The obtained results indicate that the models exhibit high stability and strong classification performance, demonstrating the effectiveness of deep learning-based methods in ship classification.

The comparative analysis of our study with recent ship classification models (summarized in Table 4) highlights that deep learning-based approaches, particularly YOLOv5 and Xception, outperform traditional machine learning models such as Random Forest (RF) and Support Vector Machines (SVM). Our 94-99% accuracy range aligns with state-of-the-art results from Chen et al. (2025) and Patel et al. (2022), both of whom employed YOLO-based architectures and achieved 99%+ classification accuracy.

Although the comparative results presented in Table 4 demonstrate the competitive performance of the proposed approach, it should be noted that the referenced studies were conducted using different datasets, image resolutions, environmental conditions, class distributions, and evaluation protocols. Therefore, direct numerical comparison between studies may have methodological limitations. Variations in dataset complexity, image quality, preprocessing techniques, and class diversity can significantly influence model performance metrics. In this context, the comparisons provided in Table 4 should be interpreted as a general performance reference rather than an absolute benchmark evaluation.

**Table 4.** Comparison of Ship Classification Methods

| Authors | Method | Results |
|---|---|---|
| Kaplan & Saray | YOLOv5 & Xception with Transfer Learning | Accuracy: 94-99% |
| Chen et al. (2025) [19] | YOLOv8x-CA-CFAR & Multi-CDT | Recall: 98.2%, F1-score: 95.8%, Classification Accuracy: 99.82% |
| Buscema et al. (2023) [20] | TOCAT (Adaptive ML Models) | Mean Accuracy: 83% |
| Kwon et al. (2024) [21] | ResNet50 + CBAM | Accuracy: 95%, Precision (Bulk Carrier: 94%, Oil Tanker: 98%), F1-score: 95% |
| Petković et al. (2023) [22] | DCNN-based Classification (SPSCD dataset) | Benchmark dataset for ship detection |
| Patel et al. (2022) [8] | YOLOv3, YOLOv4, YOLOv5 | YOLOv5: Accuracy 99%, YOLOv4: 98%, YOLOv3: 97% |
| Chen et al. (2020) [25] | DWT + DRDN | F1-score: 94.21%, Outperforms ResNet-101 (88.61%) & DenseNet-264 (92.20%) |
| Wang et al. (2019) [26] | Retina Net with FPN & Focal Loss | mAP: 97.56% (Faster R-CNN: 85.26%, SSD: 72.52%) |

One crucial point to consider in both models is that the classification of "Frigate" type ships showed lower performance in the confusion matrix and quantitative evaluation metrics compared to other ship classes. The primary reason for this is the high structural similarity among frigates, making differentiation more challenging. Kwon et al. (2024) introduced attention mechanisms using CBAM with ResNet50, which improved classification accuracy to 95%, indicating that incorporating similar strategies in future work could enhance feature extraction and classification precision.

Another notable factor affecting ship classification is the impact of environmental conditions, such as night-time images, low-resolution inputs, and small-scale ship representations. However, our quantitative evaluation metrics suggest that these factors do not significantly hinder classification accuracy within a certain threshold. To further enhance model performance, the following solutions are proposed: Increasing the dataset size to provide more diverse training examples, improving model generalization.

Incorporating Long Short-Term Memory (LSTM) layers to capture long-term dependencies within processed data, improving feature extraction and classification accuracy. Exploring attention mechanisms, similar to Kwon et al. (2024), to enhance feature selection and object recognition performance. Developing an ensemble learning framework that integrates multiple deep learning models to optimize classification accuracy and robustness. Compared to traditional machine learning methods, the use of deep learning models in this study significantly enhanced semantic feature representations, resulting in higher classification performance than similar works in the literature. The results demonstrate that YOLOv5 and Xception-based models are highly effective for ship classification, particularly in maritime surveillance and security applications.

The main contributions of this study can be summarized as follows:

A comprehensive ship image dataset was constructed using web scraping techniques from publicly available sources.

A dual-path deep learning classification framework combining raw image processing and Hilbert-Huang Transform-based feature extraction was proposed.

The effectiveness of the proposed architecture was validated using multiple evaluation metrics, including accuracy, precision, recall, F1-score, and AUC.

The integration of attention mechanisms enhanced classification performance, especially for visually similar ship classes.

Experimental results demonstrated that the proposed approach achieves high classification accuracy and provides a reliable solution for maritime surveillance and security applications.

For future research, integrating hybrid deep learning architectures and leveraging attention-based models may further improve classification accuracy, ensuring more reliable and efficient ship classification frameworks in real-world maritime operations. Although the integration of CBAM has significantly improved classification accuracy and reduced inter-class confusion, future research may explore the application of more recent and advanced architectures. In particular, transformer-based vision models (e.g., Vision Transformers - ViTs, and hybrid CNN-transformer models) have demonstrated remarkable success in capturing global contextual information in complex visual tasks. Moreover, state-of-the-art object detection architectures such as YOLOv9 offer high-speed, real-time performance while maintaining high precision, and could be explored for multi-class ship detection tasks under varying resolution and noise conditions.

Integrating these newer models could further enhance the model's ability to distinguish between visually similar ship types and adapt to diverse maritime environments. Comparative studies between CBAM-enhanced CNNs and these next-generation models would provide deeper insights into model efficiency, robustness, and generalization capabilities.

**Peer-review:** External, Independent.

**Acknowledgements:**
The authors would like to thank all institutions and publicly available data sources that contributed to the development of the dataset used in this study. No additional acknowledgements are declared.

**Declarations:**

***1. Statement of Originality:***
The authors declare that this manuscript is original, has not been published previously, and is not under consideration for publication elsewhere. All sources, datasets, and references used in this study have been appropriately cited.

***2. Author Contributions:***
***Concept:*** YK,US; ***Conceptualization:*** YK,US; ***Literature Search:*** YK,US; ***Data Collection:*** YK,US; ***Data Processing:*** YK,US; ***Analysis:*** YK,US; ***Writing – original draft:*** YK,US; ***Writing – review & editing:*** YK,US.

***3. Ethics approval:***
This study does not involve human participants, animal subjects, clinical data, or personally identifiable information. The dataset used in this research was created from publicly available ship images collected through web scraping from open sources. Therefore, ethical committee approval was not required.

***4. Funding/Support:***
The authors received no specific financial support, grant, or funding for this research.

***5. Competing Interests:***
The authors declare no competing interests.

***6. GenAI Usage Statement:***
No GenAI tools were used at any stage of the study.

***7. Sustainable Development Goals:***


## REFERENCES

[1] Yang, S., Cao, Z., Liu, N., Sun, Y., Wang, Z. 2024. Maritime Electro-Optical Image Object Matching Based on Improved YOLOv9. Electronics, 13(14), 1-16.

[2] Javed, M. F., Imam, M. O., Adnan, M., Murtza, I., Kim, J. Y. 2024. Maritime Object Detection by Exploiting Electro-Optical and Near-Infrared Sensors Using Ensemble Learning. Electronics, 13(18), 3604.

[3] Wang, L. vd. 2021. A Review of Methods for Ship Detection with Electro-Optical Images in Marine Environments. Journal of Marine Science and Engineering, 9(12), 1351.

[4] Zhao, T. vd. 2024. Ship Detection with Deep Learning in Optical Remote-Sensing Images: A Survey of Challenges and Advances. Remote Sensing, 16(7), 1185.

[5] Yu, M., Han, S., Wang, T., Wang, H. 2022. An Approach to Accurate Ship Image Recognition in a Complex Maritime Transportation Environment. Journal of Marine Science and Engineering, 10(12), 1840.

[6] Wang, Y., Wang, C., Zhang, H. 2018. Ship Classification in High-Resolution SAR Images Using Deep Learning of Small Datasets. Sensors, 18(9), 2929.

[7] Kim, K., Hong, S., Choi, B., Kim, E. 2018. Probabilistic Ship Detection and Classification Using Deep Learning. Applied Sciences, 8(6), 936.

[8] Patel, K., Bhatt, C., Mazzeo, P. L. 2022. Deep Learning-Based Automatic Detection of Ships: An Experimental Study Using Satellite Images. Journal of Imaging, 8(7), 179.

[9] Gupta, H., Verma, O. P., Sharma, T. K., Varshney, H., Agarwal, S., Pak, W. 2024. Ship Detection Using Ensemble Deep Learning Techniques from Synthetic Aperture Radar Imagery. Scientific Reports, 14, 1963.

[10] Yang, J., Zheng, Y., Xu, W., Sun, P., Bai, S. 2024. An Accurate and Robust Multimodal Template Matching Method Based on Center-Point Localization in Remote Sensing Imagery. Remote Sensing, 16(15), 2765.

[11] Lowe, D. G. 2004. Distinctive Image Features from Scale-Invariant Keypoints. International Journal of Computer Vision, 60(2), 91-110.

[12] Dolapci, B., Özcan, C. 2021. Automatic Ship Detection and Classification Using Machine Learning from Remote Sensing Images on Apache Spark. Journal of Intelligent Systems: Theory and Applications, 4(1), 94-102.

[13] Wang, P. vd. 2023. Understanding Deep Representation Learning via Layerwise Feature Compression and Discrimination. arXiv:2311.02960. http://arxiv.org/abs/2311.02960 (Erişim Tarihi: 25.03.2025).

[14] Kaya, M., Ulutürk, S., Çetin Kaya, Y., Altıntaş, O., Karaca, Y. 2023. Optimization of Several Deep CNN Models for Waste Classification. Sakarya University Journal of Computer and Information Sciences, 6(2), 91-104.

[15] Shi, Q., Li, W., Tao, R., Sun, X., Gao, L. 2019. Ship Classification Based on Multifeature Ensemble with Convolutional Neural Network. Remote Sensing, 11(4), 419.

[16] Ramakrishnan, P., Sivagurunathan, P. T., Kumar, N. S. 2019. Fruit Classification Based on Convolutional Neural Network. International Journal of Control and Automation, 12(6), 232-239.

[17] Jiang, P., Ergu, D., Liu, F., Cai, Y., Ma, B. 2021. A Review of YOLO Algorithm Developments. Procedia Computer Science, 199, 1066-1073.

[18] Woo, S., Park, J., Lee, J. Y., Kweon, I. S. 2018. CBAM: Convolutional Block Attention Module. Proceedings of the European Conference on Computer Vision, 3-19.

[19] Chen, L., Hu, Z., Chen, J., Sun, Y. 2025. SVIADF: Small Vessel Identification and Anomaly Detection Based on Wide-Area Remote Sensing Imagery and AIS Data Fusion. Remote Sensing, 17(2), 336.

[20] Buscema, P. M., Massini, G., Raimondi, G., Caporaso, G., Breda, M., Petritoli, R. 2023. A Pattern Recognition Analysis of Vessel Trajectories. Algorithms, 16(9), 420.

[21] Zhang, T., Zhang, X., Shi, J., Wei, S. 2019. Balance Scene Learning Mechanism for Ship Detection in Optical Remote Sensing Images. IEEE Transactions on Geoscience and Remote Sensing, 57(7), 4645-4658.

[22] Petković, M., Vujović, I., Lušić, Z., Šoda, J. 2023. Image Dataset for Neural Network Performance Estimation with Application to Maritime Ports. Journal of Marine Science and Engineering, 11(3), 487.

[23] Yang, Z., Lai, Y., Zhou, H., Tian, Y., Qin, Y., Lv, Z. 2023. Improving Ship Detection Based on Decision Tree Classification for High Frequency Surface Wave Radar. Journal of Marine Science and Engineering, 11(3), 541.

[24] Yan, Z., Song, X., Zhong, H., Yang, L., Wang, Y. 2022. Ship Classification and Anomaly Detection Based on Spaceborne AIS Data Considering Behavior Characteristics. Sensors, 22(20), 7848.

[25] Chen, L., Shi, W., Fan, C., Zou, L., Deng, D. 2020. A Novel Coarse-to-Fine Method of Ship Detection in Optical Remote Sensing Images Based on a Deep Residual Dense Network. Remote Sensing, 12(19), 3112.

[26] Wang, Y., Wang, C., Zhang, H., Dong, Y., Wei, S. 2019. Automatic Ship Detection Based on RetinaNet Using Multi-Resolution Gaofen-3 Imagery. Remote Sensing, 11(5), 531.

[27] Choi, K., Yi, J., Park, C., Yoon, S. 2021. Deep Learning for Anomaly Detection in Time-Series Data: Review, Analysis and Guidelines. IEEE Access, 9, 120043-120065.

[28] Li, J., Du, X., Martins, J. R. R. A. 2022. Machine Learning in Aerodynamic Shape Optimization. Progress in Aerospace Sciences, 134, 100849.

[29] Azam, Z., Islam, M. M., Huda, M. N. 2023. Comparative Analysis of Intrusion Detection Systems and Machine Learning-Based Model Analysis Through Decision Tree. IEEE Access, 11, 80348-80391.

[30] Ali, S. vd. 2023. Explainable Artificial Intelligence (XAI): What We Know and What Is Left to Attain Trustworthy Artificial Intelligence. Information Fusion, 99, 101805.

[31] Baduge, S. K. vd. 2022. Artificial Intelligence and Smart Vision for Building and Construction 4.0: Machine and Deep Learning Methods and Applications. Automation in Construction, 141, 104440.

[32] Shafiq, M., Gu, Z. 2022. Deep Residual Learning for Image Recognition: A Survey. Applied Sciences, 12(18), 8972.

[33] Cuomo, S., Di Cola, V. S., Giampaolo, F., Rozza, G., Raissi, M., Piccialli, F. 2022. Scientific Machine Learning Through Physics-Informed Neural Networks: Where We Are and What's Next. Journal of Scientific Computing, 92(3), 81.

[34] Tan, M., Le, Q. V. 2019. EfficientNet: Rethinking Model Scaling for Convolutional Neural Networks. Proceedings of the International Conference on Machine Learning, 6105-6114.

[35] He, K., Zhang, X., Ren, S., Sun, J. 2016. Deep Residual Learning for Image Recognition. Proceedings of IEEE Conference on Computer Vision and Pattern Recognition, 770-778.

[36] Fakhrabadi, A. K., Shahbazzadeh, M. J., Jalali, N., Eslami, M. 2025. A Hybrid Inception-Dilated-ResNet Architecture for Deep Learning-Based Prediction of COVID-19 Severity. Scientific Reports, 15, 6490.

[37] Isohanni, J. 2025. Customised ResNet Architecture for Subtle Color Classification. International Journal of Computer Applications, 187(21), 7-12.

[38] Mondal, M. K., Debnath, S. 2025. HHT Based Protection for Series Compensated Double Circuit Transmission Lines Considering Evolving and Cross-Country Faults. Engineering Research Express, 7(1), 015003.

[39] Bowman, D. C., Lees, J. M. 2013. The Hilbert-Huang Transform: A High Resolution Spectral Method for Nonlinear and Nonstationary Time Series. Seismological Research Letters, 84(6), 1074-1080.

[40] Dong, R., Cai, D., Asai, N. 2017. Nonlinear Dance Motion Analysis and Motion Editing Using Hilbert-Huang Transform. Proceedings of the 2017 ACM International Conference on Computer Graphics and Interactive Techniques in Australasia and Southeast Asia, 1-4.